UNIVERSITY of
BRADFORD

Library

The University of Bradford Institutional Repository

http://bradscholars.brad.ac.uk

This work is made available online in accordance with publisher policies. Please refer to the repository record for this item and our Policy Document available from the repository home page for further information.

To see the final version of this work please visit the publisher's website. Access to the published online version may require a subscription.

Link to publisher's version: *https://doi.org/10.1007/s13203-018-0201-1*

Citation: John YM, Patel R and Mujtaba IM (2018) Maximization of propylene in an industrial FCC unit. Applied Petrochemical Research. 8(2): 79-95.

ORIGINAL ARTICLE

Maximization of propylene in an industrial FCC unit

Yakubu M. John[1] · Raj Patel[1] · Iqbal M. Mujtaba[1]

Abstract

The FCC riser cracks gas oil into useful fuels such as gasoline, diesel and some lighter products such as ethylene and propylene, which are major building blocks for the polyethylene and polypropylene production. The production objective of the riser is usually the maximization of gasoline and diesel, but it can also be to maximize propylene. The optimization and parameter estimation of a six-lumped catalytic cracking reaction of gas oil in FCC is carried out to maximize the yield of propylene using an optimisation framework developed in gPROMS software 5.0 by optimizing mass flow rates and temperatures of catalyst and gas oil. The optimal values of 290.8 kg/s mass flow rate of catalyst and 53.4 kg/s mass flow rate of gas oil were obtained as propylene yield is maximized to give 8.95 wt%. When compared with the base case simulation value of 4.59 wt% propylene yield, the maximized propylene yield is increased by 95%.

List of symbols

A	Surface area (m^2)
A_{ptc}	Effective interface heat transfer area per unit volume (m^2/m^3)
C	Mole concentration (kg mol/m^3)
C_{p_g}	Gas heat capacity (kJ/kg K)
C_{p_s}	Solid heat capacity (kJ/kg K)
D	Diameter (m)
d_c	Catalyst average diameter (m)
E	Activation energy (kJ/kg mol)
F	Mass flow rate (kg/s)
H	Specific enthalpy (kJ/kg)
ΔH	Heat of reaction (kJ/kg)
ΔH_{vlg}	Heat of vaporization of liquid feedstock in the feed vaporization section (kJ/kg)
h	Enthalpy of reaction (kJ/kg)
h_p	Interface heat transfer coefficient between the catalyst and gas phases
h_T	Interface heat transfer coefficient (kJ/m^2 s K)
k_{i0}	Frequency factor in the Arrhenius expression (1/s)
K_i	Rate coefficient of the four-lump cracking reaction (1/s)
K_g	Thermal conductivity of hydrocarbons
L	Length (m)
M_w	Molecular weight
P	Pressure (kPa)
Q_{react}	Rate of heat generation or heat removal by reaction (kJ/s)
R	Ideal gas constant (8.3143 kPa m^3/kg mol K or kJ/kg mol K)
RAN	Aromatics-to-naphthenes ratio in liquid feedstock
S_c	Average sphericity of catalyst particles
S_g	Total mass interchange rate between the emulsion and bubble phases (1/s)
T	Temperature (K)
u	Superficial velocity (m/s)
V	Volume (m^3)
Y_{cc}	Weight fraction of Conradson carbon residue in a feedstock
y	Weight fraction
Z	Gas compressibility factor or Z factor

Greek symbols

Ω	Cross-sectional area
ρ	Density (kg/m^3)
$\varnothing$	Catalyst deactivation function
ε	Voidage
α	Catalyst deactivation coefficient
α_C^*	Exponent for representing α
μ_g	Viscosity

✉ Iqbal M. Mujtaba
 I.M.Mujtaba@bradford.ac.uk

[1] Chemical Engineering Division, School of Engineering, University of Bradford, Bradford BD7 1DP, UK

Subscripts

cc	Coke on catalyst
cL1	Cyclone 1
ck	Coke
c4	Butylene
c3	Propylene
ds	Disperse steam
FS	Feed vaporization section
g	Acceleration (m/s^2)
gl	Gasoline
g	Gas
go	Gas oil
dg	Dry gas
MABP	Molal average boiling temperature (K)
MeABP	Mean average boiling temperature (K)
pc	Pseudo-critical
pr	Pseudo-reduced
RS	Riser
RT	Disengager-stripping section

Introduction

The fluid catalytic cracking (FCC) is one of the most important refining processes within an oil refinery [1]. It is a key technology that converts heavy distillates, such as bottoms of vacuum and atmospheric distillation units, into desirable products such as gasoline, diesel and middle distillates, using zeolite-cracking catalyst [2]. These cracking reactions take place in the riser column [3]. The FCC is a type of secondary unit operation and one of the most important processes in a petroleum refinery. The FCC unit is mostly used to increase gasoline and diesel yield to meet high demand of fuel which is due to increase in transportation. However, it is not just to increase gasoline and diesel but middle distillates such as the gas lump as well, which comprises light olefins such as ethylene and propylene; major sources of the raw materials for the polyethylene and polypropylene industries. These light olefins are the most important raw materials for many chemicals such as acrylonitrile, propylene oxide, and other chemicals that are consumed as substitutes for non-plastic materials [4].

In recent times, there has been an increase in the demand for propylene, a petrochemical industry feedstock [5] and it is chiefly sourced from light olefins in the naphtha steam pyrolysis process. Naphtha steam pyrolysis process is a high energy consumption process because it is carried out at about 800 °C and separation of olefins is done at a temperature as low as −100 °C [5]. This makes the naphtha steam pyrolysis process a more capital intensive one. However, propylene and ethylene are sourced cheaply from the FCC unit due to the abundance and cheapness of the FCC feedstock compared with Naphtha [4, 5], and the recent growth

in demand for propylene in the world has maintained focus on the refineries toward FCC technologies for the maximization of propylene production to achieve economic profit [6]. In addition, the FCC operates below 550 °C and does not require extreme 'cold' for the separation of propylene from liquefied petroleum gas (LPG) [5]. Therefore, the cost of producing propylene from the FCC is much lower than that from steam pyrolysis [7]. The FCC unit is thus ideally suited for the manufacture of ethylene and propylene from the light products. Currently, there is an increasing interest in maximizing propylene yield of FCC units [7, 8]. The FCC unit has the ability to produce high yields when suitable operating conditions are selected. However, due to changes in quality, nature of the crude oil feedstock, changes in the environment and the desire to achieve maximum profitability, it results in many different operating conditions in the FCC riser unit [5, 9].

According to Almeida and Secchi [10] and John et al. [9], the riser can produce large profits when it runs at maximum capacity with maximum feed rate and power applied to the equipment. Optimization of the design and operation is crucial to facilitate the constantly changing quality and nature of blends of feedstocks while meeting the maximum capacity requirements. Some factors such as the large amount of feed processed, valuable gasoline yield, gas lump yield, the various processes occurring in the riser and its economic operation affects the overall economic performance of the refinery; thus it is vital to improve the performance of the riser through process optimization strategies [9, 11].

The production of propylene is mostly achieved using catalytic reactions with special selectivity for propylene [7, 8, 12, 13]. A number of lumps for catalytic cracking were reported in the literature but most of them lumped the gaseous products in a single lump, thereby making it difficult to optimize or maximize a particular gas, for instance propylene. Usman et al. [14] conducted experiment using three different crudes (Super Light, Extra Light and Arab Light) catalytically cracked to produce light olefins, where they presented propane and propylene as different lumps. They used different catalysts: base-equilibrated catalyst and others; (Z30 and Z1500) which are the base-equilibrated catalyst + MFI Zeolite at varying Si/Al ratio. The results shows that the total weight fraction of the two lumps; propylene and propane has propylene about 80–89% for all the crude oils and catalysts used [14]. This percentage is high, therefore, a combined lump of propylene and propane can be treated as a single lump of propylene and the kinetic model of Ancheyta and Rogelio [15] is suitable for this work. Hence, in this study, the FCC riser is simulated based on a six-lumped kinetic model [15] consisting of vacuum gas oil, gasoline, C$_3$'s (propane and propene), C$_4$'s (butane and butene), dry gas (H$_2$, C$_1$–C$_2$) and coke. Vacuum gas oil is the feed whilst gasoline, butylene, propylene and dry gas are products with

coke deposited on the catalyst. The yield of the propylene is further enhanced by optimizing the operating conditions of the riser.

The FCC riser is a complex unit that involves strong multi-variable interactions, complex hydrodynamics and operating restrictions, which poses as a major difficulty in the simulation of the process. However, minimal changes due to simulation and optimization can result in higher yield, thus increasing economic benefits. In the FCC unit, the yield of propylene is influenced by the reaction temperature, catalyst-to-oil ratio (C/O), residence time, nature of feed and the catalyst system [16–18], and when any of the foregoing variables is optimized, the yield of propylene can considerably increase.

Hence, gPROMS software 5.0 will be utilized for the simulation and optimization of the riser to obtain results showing the effects of changing variables such as temperature and mass flow rates [9] on the yield of propylene. To carry out this optimization, a single objective function was developed and implemented in gPROMS software that uses a successive reduced quadratic programming (SRQPD) optimization technique. This technique is a Sequential Quadratic Programming-based solver imbedded in the gPROMS software. Hence, the aim of this work is to maximize the yield of propylene by varying different sets of riser operational conditions.

Riser model

The FCC unit (Fig. 1) houses the cylindrical vessel called riser, which is the main reactor, where the cracking reaction takes place in the presence of a catalyst. The catalyst, a mixture of crystalline alumina silicates (zeolites) is a sand-like material which is fluidized into a fluid via contact with liquid fed into the FCC unit [2, 9]. A typical configuration
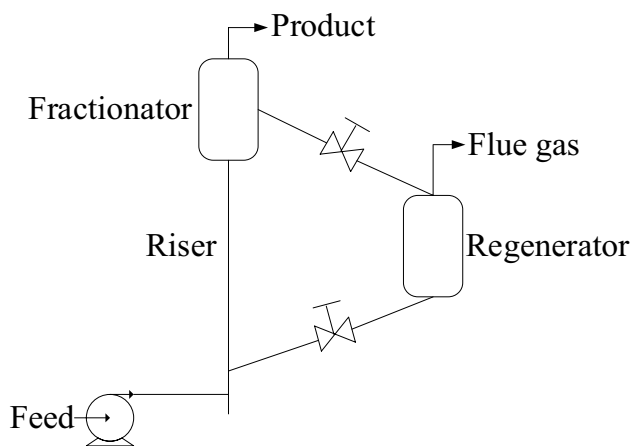

Fig. 1 A schematic diagram of the FCC unit

of a FCC process consists of two major units; the riser and regenerator.

This study is focused on the riser unit of the FCC since it is where the products are made. It is modelled as plug flow and the vaporization of gas oil was considered to be instantaneous in the vaporization section. The hot regenerated catalyst from the regenerator meets the feed at the vaporization section and vaporizes the feed with the aid of dispersion steam to move upward into the riser where the gas oil gets cracked on the catalyst and produces desirable products [2]. The riser in this work is of industrial size; 30 m high and 1.0 m diameter, whose simulation and further optimization is carried out using the mathematical models obtained from the literature [2, 19, 20] as presented in Table 1. The choice of the mathematical model is based on the fact that it captures the actual hydrodynamic model of an industrial FCC unit and has been used extensively in the literature. The riser is simulated using a six-lump kinetic model as shown in Fig. 2, and the kinetic data for the various constants in Fig. 2 are estimated using parameter estimation technique. The simulation involves many other parameters such as the feed conditions, catalyst properties and riser dimensions which were obtained from the literature and presented in Appendix Tables 8 and 9. The steady state model is derived from mass, energy and momentum balance equations for the catalyst and gaseous phases of the riser, while assuming that there is no loss of heat from the riser to the surrounding [21]. In addition, it is assumed that the cracking reactions only take place on catalyst surface.

Equations (1)–(6) represent the overall rates of reaction for gas oil; R_{go}, gasoline; R_{gl}, gas; R_{C4}, butylene; R_{C3}, propene; R_{dg}, dry gas, and R_{ck}, coke; for the six-lump kinetic reactions. Each overall rate of reaction is a function of overall rate constants, defined by the Arrhenius equation given in Eqs. (7)–(18). The rate of heat removal by reaction Q_{react} is given by Eq. (19), while Eqs. (20)–(25) and Eqs. (26)–(27) result from the material and energy balance of the catalyst and gas phases, respectively. The equations describing the hydrodynamics of the riser are Eqs. (28)–(53) [2, 19]. Equations (28) and (29) describe the catalyst and gas velocity profiles across the riser [2]. Equations (30) and (31) describe the gas volume fraction, ε_g, and catalyst volume fraction, ε_c; they provide a hydrodynamic constrain such that the summation of the volume fractions is unity. The riser pressure is described by Eq. (37), which is obtained from the simple ideal gas relationship with Z as compressibility factor [22] described in Eq. (47).

gPROMS is a robust software used for solving the set of differential algebraic equations describing the riser. It is an equation-oriented software and all solvers have been designed specifically for large-scale systems such as the FCC unit with no restrictions regarding the size of the differential–algebraic equations other than those imposed by

Table 1 Equations and descriptions

Description of variable	Equations	Eq. no.
Kinetic model equations for the six-lumped model		
Gas oil R_{go} reaction rate	$R_{go} = -(K_1 + K_2 + K_3 + K_4 + K_5)y_{go}^2\emptyset_c$	(1)
Gasoline R_{gl} reaction rate	$R_{gl} = (K_1 y_{go}^2 - K_6 y_{gl} - K_7 y_{gl} - K_8 y_{gl} - K_9 y_{gl})\emptyset_c$	(2)
Butylene R_{C4} reaction rate	$R_{C4} = (K_2 y_{go}^2 + K_6 y_{gl} - K_{10}y_{C4} - K_{11}y_{C4})\emptyset_c$	(3)
Propylene R_{C3} reaction rate	$R_{C3} = (K_3 y_{go}^2 + K_7 y_{gl} + K_{10}y_{C4} - K_{12}y_{C3})\emptyset_c$	(4)
Light gas R_{dg} reaction rate	$R_{dg} = (K_4 y_{go}^2 + K_8 y_{gl} + K_{11}y_{C4} + K_{12}y_{C3})\emptyset_c$	(5)
Coke R_{Ck} reaction rate	$R_{ck} = (K_5 y_{go}^2 + K_9 y_{gl})\emptyset_c$	(6)
Gas oil to gasoline overall rate constant	$K_1 = k_{10}\exp\left(\frac{-E_1}{RT_g}\right)$	(7)
Gas oil to butylene overall rate constant	$K_2 = k_{20}\exp\left(\frac{-E_2}{RT_g}\right)$	(8)
Gas oil to propylene overall rate constant	$K_3 = k_{30}\exp\left(\frac{-E_3}{RT_g}\right)$	(9)
Gas oil to dry gas overall rate constant	$K_4 = k_{40}\exp\left(\frac{-E_4}{RT_g}\right)$	(10)
Gas oil to coke overall rate constant	$K_5 = k_{50}\exp\left(\frac{-E_5}{RT_g}\right)$	(11)
Gasoline to butylene overall rate constant	$K_6 = k_{60}\exp\left(\frac{-E_6}{RT_g}\right)$	(12)
Gasoline to propylene overall rate constant	$K_7 = k_{70}\exp\left(\frac{-E_7}{RT_g}\right)$	(13)
Gasoline to dry gas overall rate constant	$K_8 = K_{80}\exp\left(\frac{-E_8}{RT_g}\right)$	(14)
Gasoline to coke overall rate constants	$K_9 = k_{90}\exp\left(\frac{-E_9}{RT_g}\right)$	(15)
Butylene to propylene overall rate constant	$K_{10} = k_{100}\exp\left(\frac{-E_{10}}{RT_g}\right)$	(16)
Butylene to dry gas overall rate constant	$K_{11} = k_{110}\exp\left(\frac{-E_{11}}{RT_g}\right)$	(17)
Propylene to dry gas overall rate constant	$K_{12} = k_{120}\exp\left(\frac{-E_{12}}{RT_g}\right)$	(18)
Q_{react} is the rate of heat generation or heat removal by reaction	$\begin{aligned}Q_{react} = -(&\Delta H_1 K_1 y_{go}^2 + \Delta H_2 K_2 y_{go}^2 + \Delta H_3 K_3 y_{go}^2 \\ &+ \Delta H_4 K_4 y_{go}^2 + \Delta H_5 K_5 y_{go}^2 + \Delta H_6 K_6 y_{gl} + \Delta H_7 K_7 y_{gl} \\ &+ \Delta H_8 K_8 y_{gl} + \Delta H_9 K_9 y_{gl} + \Delta H_{10} K_{10} y_{C4} \\ &+ \Delta H_{11} K_{11} y_{C4} + \Delta H_{12} K_{12} y_{C4})\emptyset_c\end{aligned}$	(19)
Riser equations from material balance		
Gas oil fractional yield	$\frac{d_{y_{go}}}{dx} = \frac{\rho_c\epsilon_c\Omega}{F_g}R_{go}$	(20)
Gasoline fractional yield	$\frac{d_{y_{gl}}}{dx} = \frac{\rho_c\epsilon_c\Omega}{F_g}R_{gl}$	(21)
Butylene fractional yield	$\frac{d_{y_{C4}}}{dx} = \frac{\rho_c\epsilon_c\Omega}{F_g}R_{C4}$	(22)
Propylene fractional yield	$\frac{d_{y_{C3}}}{dx} = \frac{\rho_c\epsilon_c\Omega}{F_g}R_{C3}$	(23)
Dry gas fractional yield	$\frac{d_{y_{dg}}}{dx} = \frac{\rho_c\epsilon_c\Omega}{F_g}R_{dg}$	(24)
Coke fractional yield	$\frac{d_{y_{ck}}}{dx} = \frac{\rho_c\epsilon_c\Omega}{F_g}R_{ck}$	(25)
Riser equations from energy balance		
Temperature of catalyst along the riser height	$\frac{dT_c}{dx} = \frac{\Omega h_p A_p}{F_c C_{pc}}(T_g - T_c)$	(26)

Table 1 (continued)

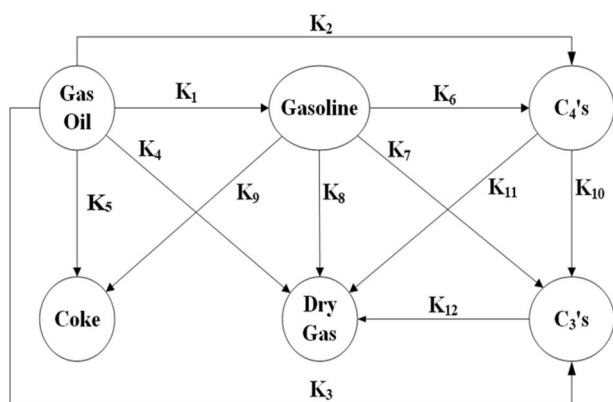| Description of variable	Equations	Eq. no.
Temperature of gas phase along the riser height	$\frac{dT_g}{dx} = \frac{\Omega}{F_g C_{pg}}[h_p A_p(T_c - T_g) + \rho_c \varepsilon_c Q_{react}]$	(27)
Riser hydrodynamic equations		
Catalyst velocity	$\frac{dv_c}{dx} = -\left(G_c \frac{\Omega}{F_c}\frac{d\varepsilon_c}{dx} + \frac{C_f(v_g - v_c)\Omega}{F_c} - \frac{2f_{rc}v_c}{D} - \frac{g}{v_c}\right)$	(28)
Gas velocity	$\frac{dv_g}{dx} = -\left(\frac{\Omega}{F_g}\frac{dP_{RS}}{dx} + \frac{C_f(v_c - v_g)}{F_g} - \frac{2f_{rg}v_g}{D} - \frac{g}{v_g}\right)$	(29)
Gas volume fraction, E_g	$\varepsilon_g = 1 - \varepsilon_c$	(30)
Catalyst volume fraction, ε_c	$\varepsilon_c = \frac{F_c}{v_c \rho_c \Omega}$	(31)
Riser cross-sectional area	$\Omega = \frac{\pi D^2}{4}$	(32)
Catalyst deactivation	$\emptyset_c = \exp(-\alpha_c C_{ck})$	(33)
Catalyst deactivation coefficient	$\alpha_c = \alpha_{c0}\exp\left(\frac{-E_c}{RT_g}\right)(R_{AN})^{\alpha_{c*}}$	(34)
Coke on catalyst	$C_{ck} = C_{ckCL1} + \frac{F_g y_{ck}}{F_c}$	(35)
Gas phase density	$\rho_g = \frac{F_g}{\varepsilon_g v_g \Omega}$	(36)
Riser pressure	$P_{RS} = \rho_g \frac{RT_g}{M_{wg}}$	(37)
Catalyst-to-oil ratio (*C/O*)	$C/O \text{ ratio} = \frac{F_c}{F_g}$	(38)
Riser pseudo-reduced temperature	$T_{pr} = \frac{T_g}{T_{pc}}$	(39)
Riser pseudo-reduced pressure	$P_{pr} = \frac{P_{RS}}{P_{pc}}$	(40)
Stress modulus of the catalyst [59]	$G_c = 10^{(-8.76\varepsilon_g + 5.43)}$	(41)
Catalyst temperature in the vaporization section	$T_{cFS} = T_{cCL1} - \frac{F_{lg}}{F_{cCL1}C_{pc}}\left[C_{plg}(T_{gFS} - T_{lg}) + \frac{F_{ds}C_{pds}}{F_{lg}}(T_{gFS} - T_{ds}) + \Delta H_{vlg}\right]$	(42)
Gas phase temperature in the vaporization section	$T_{gFS} = \frac{B_{lg}}{A_{lg} - \log(P_{FS}.y_{goFS})} - C_{lg}$	(43)
Pressure at vaporization	$P_{FS} = P_{RT} + \Delta P_{RS}$	(44)
Weight fraction of feed (gas oil) in the vaporization section	$y_{goFS} = \frac{F_{lg}}{F_{lg} + F_{ds}}$	(45)
Velocity of gas phase in the vaporization section	$v_{gFS} = \frac{F_{lg} + F_{ds}}{\rho_{gFS}(1 - \varepsilon_{cCL1})\Omega_{FS}}$	(46)
Velocity of entrained catalyst in the vaporization section	$v_{cFS} = \frac{F_{cCL1}}{\rho_c \varepsilon_{cCL1} \Omega_{FS}}$	(47)
Gas oil density in the vaporization section	$\rho_{gFS} = \frac{P_{FS} M_{wgFS}}{RT_{gFS}Z_{gFS}}$	(48)
Catalyst phase velocity	$v_{cRS}^{(0)} = v_{cFS}$	(49)
Gas phase velocity	$v_{gRS}^{(0)} = v_{gFS}$	(50)
Catalyst mass flow rate	$F_{cRS} = F_{cCL1}$	(51)
Gas phase mass flow rate	$F_{gRS} = F_{lg} + F_{ds}$	(52)
Heat of vaporization of gas oil	$\Delta H_{vlg} = 0.3843 T_{MABP} + 1.0878 \times 10^3 \exp\left(\frac{-M_{wm}}{100}\right) - 98.153$	(53)
Z factor of Heidaryan et al. [22]	$Z = \ln\left[\frac{A_1 + A_3 \ln(P_{pr}) + \frac{A_5}{T_{pr}} + A_7(\ln P_{pr})^2 + \frac{A_9}{T_{pr}^2} + \frac{A_{11}}{T_{pr}}\ln(P_{pr})}{1 + A_2 \ln(P_{pr}) + \frac{A_4}{T_{pr}} + A_6(\ln P_{pr})^2 + \frac{A_8}{T_{pr}^2} + \frac{A_{10}}{T_{pr}}\ln(P_{pr})}\right]$	(54)
Weight fraction of Coke at inlet	$y_{ck}^{(0)} = \left(\frac{F_{lg}Y_{cc}}{F_{gRS}}\right)$	(55)
Gas phase velocity	$T_c^{(0)} = T_{cFS}$	(56)
Catalyst mass flow rate	$T_g^{(0)} = T_{gFS}$	(57)

Fig. 2 Six-lump model [2, 15]

available machine memory [23]. gPROMS is a process modelling software for simulation, optimisation and control (both steady state and dynamic) of highly complex processes such as the FCC unit riser. Due to its robustness, more research work on the FCC unit is being carried out using gPROMS in recent time [9, 20, 24, 25]. These are the first attempts on the FCC unit and gPROMS displayed great capability and reliability. The riser model construction is described in the model section and the parameters are specified in the process section of the gPROMS software 5.0.0.

Riser kinetics and parameter estimation

The kinetic studies on the production of propylene have been carried out and they are mostly based on catalytic pyrolysis. However, catalytic pyrolysis includes catalytic reactions and thermal reactions [26], and the cracking extent of catalytic pyrolysis is more comprehensive than that of catalytic cracking [27]. In addition, catalytic cracking is favoured over thermal cracking for maximum propylene production especially in high severity FCC unit [18]. Moreover, just like the catalytic cracking reactions require the understanding of the kinetics of the reaction involved for reactor design, the design of the catalytic pyrolysis reactor would require the understanding of both the thermal and catalytic reactions involved to design a catalytic pyrolysis reactor. This is true because kinetic study is an essential mean for thorough understanding of reactions and catalysis for any catalysed chemical reaction which helps in the correct design of chemical reactors and determines the progress of the chemical reaction [28]. In this study, mathematical and kinetic models used are based on the kinetic-lumping approach which catalytic cracking as a form of reaction was employed [2, 9, 19].

One of the kinetic-lumped models for the production of propylene based on catalytic pyrolysis of heavy oils is

the eight-lumped model [26] which include ethylene as a lump and a separate propylene lumped with butylene. Where propylene is required as a separate lump, this eight-lumped model may not be useful. Some kinetic models for the propylene production are based on catalytic cracking, such as the four-lumped model which includes propylene as a component of a gas lump [29]; the ten-lumped model with propylene as a distinct lump [30] and six-lumped model with distinct propylene lump [15]. To maximize the yield of propylene in a lumped kinetic model, propylene has to be a separate lump. The gas lump in Hussain et al. [29] is a mixture of propylene, butylene and some dry gas; hence, it is unsuitable for use to maximize propylene because maximizing gas lump would mean maximizing other gases along.

The ten-lumped model of Du et al. [30] and six-lumped model of Ancheyta and Rogelio [15] are most suitable for their ability to have propylene as unique lumps. However, the yields of lumps were obtained at a particular constant temperature; 580 °C [30] and 500 °C [15], instead of progressive temperature profile of the catalyst and vapour phases as it is obtainable in the industrial FCC riser. Specific rate constants for the various cracking reactions and catalyst deactivation in a typical industrial riser also vary along the length of the riser. In this work, the catalyst deactivation is represented by Eq. (33) which as a function of varying temperature of the gas phase of the riser. Since temperature varies in the riser and has effect on some important kinetic variables such as rate constants and catalyst deactivation, it therefore means that heat required at every point in the riser varies. This heat requirement is estimated by heat of reaction of all cracking reactions as shown in Eq. (19).

The riser mathematical model used in this work requires kinetic data that involves activation energy, frequency factor and heat of reaction, and all vary along the riser. Hence, in this work, heats of reactions, frequency factors and activation energies for varying rate constants are estimated using parameter estimation. Where the kinetic parameters to be estimated are numerous and especially with limited laboratory data available, it poses a lot of challenges [31, 32]. For the parameter estimation and simulation of the riser, the six-lumped model [15] is chosen over the ten-lumped model because it predicts propylene as a single lump and has less parameters to be estimated which reduces the complexity of the model.

Parameter estimation

Parameter estimation is carried out for a certain model by optimizing nearly all or some parameters by means of experimental data. The optimized estimated parameters are those best matches between the experimental data and predicted data by the model [33]. There are several techniques used for

parameter estimation in chemical and biochemical engineering for systems of dynamic and steady state models [31–36]. A technique for parameter estimation is carried out through online optimization where the estimates are taken from minimization of the sum of squared errors of the optimization problem by matching the experimental and calculated results within some given range of constraints [37, 38]. This method has acceptance in the parameter estimation of chemical processes [39] and it is the method used in this work. It uses the Successive Quadratic Programming (SQP) [40] on the optimization framework of gPROMS software [41] and it is proved to be very capable [39].

gPROMS parameter estimation requires the use of experimental data for validation and for the design of experiments on the gPROMS platform. In this work, the experimental results were obtained from the literature [15] for each of the six-lumped models are used as experimental data to generate the predicted results. Ancheyta and Rogelio [15] presented 15 sets of fractional yields for the six lumps obtained at fifteen different weight hourly space velocities (WHSV) from 6 to 48 h^{-1} and at 773 K. These sets of fractional yields for the six lumps were read with a software called Webplotdigitizer 3.8 and are presented in Table 2. On the gPROMS parameter estimation framework, the fifteen sets of results are used with each set for a single experiment that represents experimental values y_i^{exp}. Along with the complete riser mathematical model (hydrodynamic, kinetic, mass and energy conservation equations), the calculated values y_i^{cal} are obtained and the sum of squared errors (SSE) are minimized.

Table 2 presents the experimental data obtained from the literature [15].

There are two approaches here: first, simulation for converging all the equality constraints and satisfying the inequality constraints; second, carrying out the optimization where the objective function is

$$\text{Obj(SSE)} = \sum_{M=1}^{M_t} (y_i^{exp} - y_i^{cal})^2, \tag{58}$$

where y is the mass fraction of lumps and i is the various lumps in the riser.

The parameter estimation problem statement can be written as

Given	The fixed riser reactor configuration, feed quality and characteristics, catalyst properties and process operational conditions
Optimize	The kinetic parameters; activation energies E, heat of reactions ΔH and frequency factors k_o at given process conditions
So as to minimize	The sum of squared errors (SSE)
Subject to	Equality and inequality constraints

Mathematically,

$$\min_{\xi_{i0}, \eta_i, \theta_i} \text{SSE},$$

s. t.

Table 2 Six-lumps yield used as experimental data

WHSV (h^{-1})	Propylene (C$_3$'s) (wt%)	Butylene (C$_4$'s) (wt%)	Gas oil (wt%)	Gasoline (wt%)	Dry gas (wt%)	Coke (wt%)
6	5.38	9.49	23.63	55.19	1.81	4.55
7	5.03	9.15	24.88	55.11	1.63	4.34
10	4.80	8.80	26.16	54.58	1.44	4.20
11	4.94	8.80	26.59	53.96	1.51	4.20
13	4.87	8.66	27.76	53.91	1.40	4.18
15	4.77	8.50	28.54	53.34	1.37	4.09
16	4.75	8.36	28.85	53.12	1.33	4.08
20	4.63	8.27	30.17	52.96	1.28	4.04
24	4.56	8.08	31.02	52.19	1.23	4.01
28	4.45	8.08	31.80	51.62	1.16	3.92
32	4.40	7.82	31.95	51.58	1.09	3.82
36	4.35	7.68	32.02	51.19	1.09	3.87
40	4.28	7.75	32.25	51.26	1.06	3.89
44	4.26	7.52	32.64	50.85	0.99	3.91
48	4.23	7.50	32.55	50.85	0.99	3.93
Average	4.65	8.30	29.39	52.78	1.29	4.07
Range	4.23–5.39	7.50–9.49	23.63–32.55	50.85–55.19	0.99–1.81	3.82–4.55

$$f(x, z'(x), z(x), u(x), v) = 0 \quad \text{(model equations, equality constraints)},$$
$$\tag{59}$$

$$\xi^l \leq \xi \leq \xi^u \quad \text{(inequality constraints)}, \tag{60}$$

$$\eta^l \leq \eta \leq \eta^u \quad \text{(inequality constraints)}, \tag{61}$$

$$\theta^l \leq \theta \leq \theta^u \quad \text{(inequality constraints)}, \tag{62}$$

where $f(x, z'(x), z(x), u(x), v) = 0$ is the model equation, x is the height of the riser and the independent variable, $u(x)$ is the decision variable; ξ is the upper and lower limits of the frequency factors k_{oi}; η is the upper and lower limits of the activation energies E_i; θ is the upper and lower limits of the heat of reactions ΔH_i. $z(x)$ is the differential and algebraic equations while $z'(x)$ is their derivative and v is the constant parameters.

Upper and lower limits are set for the decision variables which of course they are the parameters requiring to be estimated. They are set based on the assumption that the kinetic values will be within the range found in the literature for four-, five- and six-lumped models. Moreover, six-lumped model was derived based on the sequential strategy [42]. They assumed that the major reactant and products of the cracking reactions have similar rate constants, hence derived the four-lumped model from the three-lumped model and hence the six-lumped model from the five-lumped model in a sequential strategy. Therefore, it is expected in this work that the upper and lower limits for the activation energy, heat of reaction and frequency factors should be within the existing range. The values from the literature are: activation energy (31,923–57,278.96 kJ/kg mol) [43, 44] and (31,820–66,570 kJ/kg mol) [19], heat of reaction (195–745 kJ/kg) and frequency factor (0.000629–1457.5 s^{-1}) [19]. The upper and lower limits are opened further wide on the gPROMS parameter estimation framework to allow the software make the best estimates. Hence, the upper and lower limits for the following variables are activation energy (0 and 100,000 kJ/kg mol), heat of reaction (0 and 1000 kJ/kg), and frequency factors (0 and 2000 s^{-1}). Another reason for opening the limits of the decision variables is to allow for the adjustment of data obtained from the laboratory model to get modified since they are being used on a mathematical model that represents an industrial unit [30].

FCC riser optimization

During optimisation, one tries to minimize or maximize a global characteristic of a process such as cost and time by exploiting the degrees of freedom under a set of constraints [33]. Therefore, it can be said that effective optimisation is needed to achieve the best process possible, in terms of obtaining more of a desired product. Optimisation can be

described by a procedure, or set of procedures to find the best optimal solution for a particular problem. Common examples include maximizing the yield from a chemical reaction [9, 33] or minimizing the amount of energy consumed in a particular process [33].

An optimisation study of a FCC unit was carried out using genetic algorithm by [45]. It was a multi-variable-multi-objective optimization technique in which a three-objective function optimisation was carried out. It included the maximization of the gasoline yield, minimisation of the air flow rate and minimisation of CO in the flue gas. This technique works by the principle of a population being generated within the upper and lower limits of the decision variables. Thereafter, an individual is selected from the population depending on their "fitness". This individual is then copied to formulate a new generation until a global maximum or minimum is found. Results obtained showed good stability but computational times were found to be very long. A dynamic real-time optimisation study of a FCC unit was carried out [10]. They developed a NLP problem and was solved using a simultaneous strategy where a continuous problem was converted into an NLP. The solution included the use of DAE system being converted into a system of algebraic equations. Results obtained matched plant data very closely. A real-time optimisation strategy for an FCC unit controller was presented [10], where a linear model predictive controller was optimized so that it would be able to handle disturbances in the commissioning or load disturbance phases. The objective function in their work was to maximize the production of LPG. Results had shown that the dynamic response of the controller was smooth and fast in the real controller and there were major issues with the controller response. John et al. [9] undertook a study to maximize the gasoline output in a FCC unit using SQP on gPROMS. The objective function was the maximization of the yield of gasoline and the variables being optimized were mass flow rates of catalyst and gas oil and temperatures of catalyst and gas phases. Their results showed a feasible solution, whereby yield of gasoline had increased by 4.51%. Another SQP algorithm was used to maximize propylene yield in a secondary reaction and 16.68 vol% was achieved [46].

With respect to the FCC process, it is obvious that the optimisation of the process can yield significant gains in different areas such as maximizing the yield of the product. Furthermore, optimisation of FCC riser can be undertaken to minimize the operating cost as well as the capital cost if observed from a design standpoint. It can also be used to minimize certain outputs such as carbon dioxide emissions to meet legislations [25]. Due to the complex nature of the FCC process, very few simulation optimisation studies have been carried out and optimisation of FCC units have been primarily through experimental means. However, the

optimisation of the process through mathematical models is now gaining grounds in research. As computers become more powerful, it is now becoming possible to undertake rigorous models of the FCC unit through first principle modelling and empirical correlations. The benefit of using these numerical optimisation models is that the costs involved are very small compared to utilising lab scale experiments as well as the speed of computation once a model is built.

There are three main issues called the constraint triangle for maximizing propylene production; the effects of existing FCC technology, operation variables and catalysts on product quality and quantity [47]. Since the alteration of the FCC unit configuration and catalyst development is not the focus of this work, even though they are very important in FCC unit optimization, only the operation variables are manipulated to maximize the yield of propylene lump (C_3's). Higher propylene production comes at the expense of gasoline. For traditional refiners, maximizing gasoline yield is more important than the propylene yield, while for those interested in petrochemical applications, the target is operating at maximum propylene yield [7].

Optimization problem statement

Optimisation of the yield of propylene.

The optimization problem can be described as

Given	The fixed volume of the riser
Optimize	The mass flow rate of catalyst, mass flow rate of gas oil and temperatures of gas and catalyst phases
So as to maximize	The yield of propylene lump (C_3's) y_{C3}
Subject to	Constraints on the mass flow rates of catalyst and gas oil, temperatures of gas and catalyst phases, and exit concentration of gasoline

The optimisation problem can be written mathematically as

Objective function:
$$\underset{T_j, FF_j, y_{gl}}{\text{Max}}\ y_{C3}. \tag{63}$$

Subject to

Process model: $f(x, \dot{z}(x), z(x), u(x), v) = 0,$ (64)

Boundary: $x = x^{max},$ (65)

Inequality constraints: $FF_g^{min} \le FF_g \le FF_g^{max}$ (66)

$FF_c^{min} \le FF_c \le FF_c^{max}$ (67)

$T_g^{min} \le T_g \le T_g^{max}$ (68)

$T_c^{min} \le T_c \le T_c^{max},$ (69)

Equality constraints: $y_{gl}^{min} \le y_{gl}.$ (70)

The entire DAE model equations can be written in a compact form as

$f(x, \dot{z}(x), z(x), u(x), v) = 0$, where x is the independent variable which in this case is the height of riser, $z(x)$ is the set of all state variables, $\dot{z}(x)$ is the derivatives of $z(x)$ with respect to the height of the riser, $u(x)$ is the vector of control variables (mass flow rates of feed and catalyst) and v is a vector of invariant parameters, such as design variables (riser diameter and height). In addition, y_{C3} is the objective function which is the yield of propylene, the desired product to be maximized in the riser. T_c is the catalyst phase temperature, T_g is the gas phase temperature, FF_g is the mass flow rate of gas oil, FF_c is the mass flow rate of catalyst, x is the height of the riser, x^{max} is the maximum riser height (30 m) and y_{gl} is the yield of gasoline. y_{gl}^{min} is the minimum value of gasoline to be maintained while propylene is maximized. T_c^{min} and T_c^{max} are the minimum and maximum bounds of the catalyst phase temperature ($700 \le T_c \le 1000$ K) and T_g^{min} and T_g^{max} are the minimum and maximum bounds of the gas phase temperature ($520 \le T_g \le 800$ K). FF_c^{min} and FF_c^{max} are the minimum and maximum bounds of the mass flow rate of catalyst ($20 \le FF_c \le 500\ \frac{kg}{s}$) and FF_g^{min} and FF_g^{max} are the minimum and maximum bounds of the mass flow rate of gas oil ($10 \le FF_g \le 100 \frac{kg}{s}$). x^{max} is the fixed height of the riser; 30 m, and y_{gl} is the minimum allowable limit for gasoline $0.40 < Y_{gl}$.

The boundaries for the mass flow rates of gas oil and catalyst are chosen such that it reflects the typical industrial FCC unit limits for C/O ratios of 4:1–10:1 by weight [48], Sadeghbeigi [49], [9]. C/O ratios for propylene production in high severity units and riser-downer are higher [18] than the C/O ratios used in conventional FCC units, which vary between 1 and 6 [16, 29, 50] and 3–25. Hence, the boundaries for the mass flow rates are open wide enough to accommodate low and high C/O ratios (1–25) on the optimization framework.

Case studies

Case 1: Optimizing catalyst mass flow rate FF_c between 20 and 500 kg/s; gas oil temperature, T_g (520–800 K); catalyst temperature, T_c (700–1000 K), while gas oil mass flow rate, FF_g, is kept constant at 58.02 kg/s.

Case 2: Optimizing gas oil mass flow rate FF_g between 20 and 500 kg/s; gas oil temperature, T_g (520–800 K); catalyst temperature, T_c (700–1000 K), while the catalyst mass flow rate, FF_c, is kept constant at 134.94 kg/s.

Case 3: Optimizing catalyst mass flow rate FF_c between 20 and 500 kg/s; gas oil temperature, T_g (520–800 K); catalyst temperature, T_c (700–1000 K); and gas oil mass flow rate FF_g between 20 and 500 kg/s.

Since FCC's major goal is the production of gasoline, a minimum of 40 wt% of gasoline is imposed as a constraint on all the optimization cases, else most of the gasoline will deplete due to secondary cracking. The choice of 40 wt% is based on the average gasoline yield presented in the literature; 44.13–45.65 wt% [51], 44 wt% [21, 52] and 40 wt% [53].

Results and discussion

Model validation and parameter estimation results

The reason for presenting the simulation results is to determine the capability of gPROMS in handling complex nonlinear DAEs of the riser using the kinetic model of Ancheyta and Rogelio [15], and to compare the simulated results obtained with those predicted results of the same kinetic model obtained experimentally by Ancheyta and Rogelio [15]. Even though the experimental results were obtained at 773 K, the simulated riser temperature was progressive along the length of the riser.

The mass flow rates for gas oil and catalyst used in this simulation are 51.8 kg/s and 190.9 kg/s, respectively, while the C/O ratio is 3.685. These mass flow rates predicted the yields of the six lumps in the range presented by Ancheyta and Rogelio [15] while the parameter estimation was carried out. The estimated kinetic parameters are presented in Table 3.

When gas oil meets the catalyst, it begins to crack to form gasoline, butylene, propylene, dry gas and coke. In this study, the cracking reaction takes place at gas oil inlet temperature of 523.0 K at the vaporization section rising to 719.9 K at the first 6 m height of the riser and levelling out for the remaining height of the riser with 706.2 K as the exit temperature. The inlet temperature of catalyst from the cyclone is 1010 K which mixes with regenerated catalyst in the vaporization section to have the catalyst temperature

Table 3 New kinetic parameters estimated

| Rate constant	Frequency factors (s^{-1})	Activation energy (kJ/ kg mol)	Heat of reaction (kJ/ kg)
$k1$	1233.51	45,005.4	284.151
$k2$	841.36	66,364.1	22.452
$k3$	1333.60	62,582.7	103.432
$k4$	6.019	66,568.4	25.596
$k5$	0.493	66,054.1	194.867
$k6$	26.056	35,760.4	675.894
$k7$	63.008	66,426.2	645.963
$k8$	8.19×10^{-6}	62,591.5	250.896
$k9$	12.048	36,983.7	565.387
$k10$	1367.37	60,938.7	496.002
$k11$	1359.88	57,575.9	899.319
$k12$	8.19×10^{-6}	45,880.0	682.498
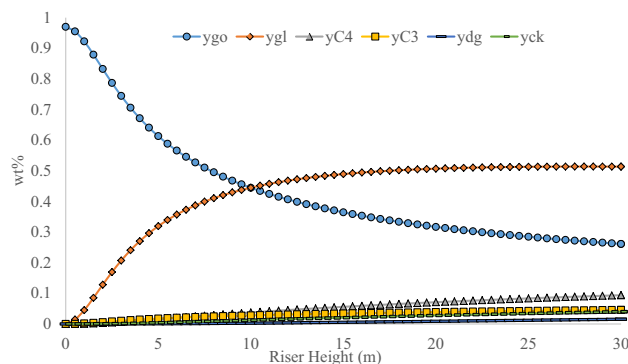
Fig. 3 Lumps of gas oil cracking

come to 971.4 K at the entrance of the riser. Cracking reactions begin immediately at the riser entrance and the profiles of these cracking reactions are presented in Fig. 3, while the temperature profiles are presented in Fig. 4.

The feed in this study is a 97.00 wt% gas oil and the remaining 3.00 wt% is steam. Figure 3 shows that the fraction of gas oil at the exit of the riser is 26.12 wt% which is 26.93% of gas oil unconverted. It also shows that about 73.07% of gas oil was consumed and about 70% of the fraction is consumed in the first 20 m of the riser. In the literature result [15], the fraction of gas oil at the exit of the riser was presented as a range because it was obtained at varied WHSV, and it is between 23.50 and 32.50 wt% which corresponds to 67.5–76.5% of gas oil consumed. The value of 26.93 wt% of unconverted gas oil obtained in this simulation at C/O ratio of 3.685 falls within the range of results from Ancheyta and Rogelio [15].
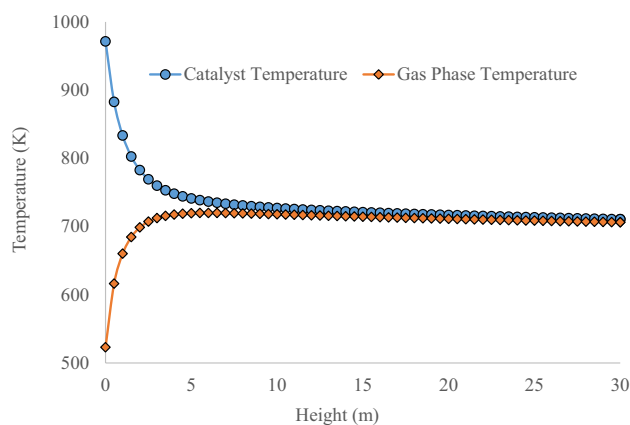
Fig. 4 Temperature profile across the riser

Likewise, gasoline started yielding as soon as cracking starts at the entrance of the riser. It rises from 0 to 51.36 wt% at the exit of the riser. This accounts for 52.95% of the total product of the riser with about 80% of the gasoline formed in the first 20 m of the riser. The value of 51.36 wt% of gasoline yield in this simulation is within the range of 50.85–55.19 wt% presented by Ancheyta and Rogelio [15].

The butylene lump (C_4's) rises from 0 to 9.39 wt% at the exit of the riser. This accounts for 9.68% of the total product of the riser and it is within the range of 7.50–9.49 wt% presented by Ancheyta and Rogelio [15].

Similarly, the propylene lump (C_3's), which is of more interest in this work, also builds up as cracking commences at the riser entrance from 0 to 4.59 wt% at the exit of the riser, accounting for 4.73 wt% of total riser products. The propylene yield of 4.80 wt% is also within the range of 4.23–5.38 wt% presented by Ancheyta and Rogelio [15] and others in the literature [54].

The dry gas lump also rises from 0 to 1.55 wt% at the exit of the riser. This is 1.60 wt% of the total product of the riser and it is within the range of 0.99–1.81 wt% presented by Ancheyta and Rogelio [15]. The remainder being coke deposited on the catalyst which also rises from 0 to 0.0399 wt% and it represents 4.11 wt% of the total product of the riser. It is also found within the range of 3.82–4.55 wt% presented by Ancheyta and Rogelio [15].

In general, the yields of the six lumps are within the range presented by Ancheyta and Rogelio [15]. This shows that the estimated kinetic parameters are true representation of the cracking reactions. The values also show that the experimental data of Ancheyta and Rogelio [15] can actually be used for the parameter estimation and the estimated kinetic parameters are useful for simulation of industrial riser. The profiles of the reactant and products are qualitatively consistent with those found in the literature [9, 19].

As cracking takes place, the endothermic reaction gives up heat from the catalyst to the gaseous phase. The endothermic heat which is determined in this simulation with the aid of the heat of reaction estimated is represented by the profile of the gas phase temperature and shown along with the profile of the catalyst phase temperature in Fig. 4. The temperature of the catalyst phase is about 971.4 K at the entrance of the riser but decreases for the first 5 m and then essentially levels out. The temperature profile of the gas phase at the entrance of the riser is about 523.0 K but rises to a maximum in the first 5 m of the riser and levels out to the exit of the riser. Both profiles start with a difference of about 448.5 K at the entrance of the riser and came so close to the same value with temperature difference of about 4.4 °C at the exit of the riser.

This temperature difference is required to accomplish the endothermic reaction. The temperature of the cracking reactions in Ancheyta and Rogelio [15] experimental work is 773 K. This temperature was reached at the riser entrance where both catalyst and oil mixed vigorously. However, the temperature of cracking in a typical riser varies at the entrance to the exit because the reaction is progressive at varied temperatures along the riser as seen in Fig. 4. The temperature profiles obtained in this work are similar to those obtained in many literatures [19, 21, 55].

Table 4 shows the comparison of the results obtained in this simulation at C/O ratio 3.685, already presented in Figs. 3 and 4, with the results presented by Ancheyta and Rogelio [15] experimental work. All the results are within the corresponding range for each lump which validates the results obtained. With an increment of 50 kg/s of catalyst mass flow rate, the C/O ratio was varied and the results are also presented for C/O ratios of 4.651, 5.616 and 6.581 in Table 4.

The unconverted gas oil yields at the varied C/O ratios are outside and lower than the range of the results by Ancheyta and Rogelio [15]. This is expected because increasing the C/O ratio increases gas oil conversion as a result of increase in cracking temperature. The absolute difference between the simulated results (C/O = 3.685) and the varied C/O ratios (C/O = 4.651, 5.616 and 6.581) shows decrease for both gas oil and gasoline. All other lumps increase due to increase in the C/O ratio and eventual rise in cracking temperature which increases the conversion of the cracking reaction. Gasoline undergoes secondary cracking to add to the butylene, propylene and dry gas lumps with additional coke deposit on the catalyst. This trend shows that increasing the C/O ratio may favour the yield of the light products such as butylene, propylene and dry gas. However, the absolute difference for propylene (5.46 wt%) at C/O ratio of 6.581 is more than that of butylene (4.31 wt%), which suggest that it would be necessary to operate the riser at C/O ratio of 6.581 to have more propylene in the light components. To get the best operating condition for propylene yield, optimization of the unit is necessary.

Table 4 Comparing simulated riser output with that of Ancheyta and Rogelio [15]

Lump (wt%)	Output range [15]	Riser output (wt%)						
		$C/O = 3.685$	$C/O = 4.651$	Difference	$C/O = 5.616$	Difference	$C/O = 6.581$	Difference
Gas oil (wt%)	23.63–32.55	26.11	19.50	− 6.61	15.58	− 10.53	13.06	− 13.05
Gasoline (wt%)	50.85–55.19	51.36	49.69	− 1.67	46.40	− 4.96	42.86	− 8.5
Butylene (C_4's) (wt%)	7.50–9.49	9.39	12.06	2.67	13.37	3.98	13.70	4.31
Propylene (C_3's) (wt%)	4.23–5.39	4.59	6.37	1.78	8.22	3.63	10.05	5.46
Dry gas (wt%)	0.99–1.81	1.55	3.36	1.81	5.58	4.03	7.92	6.37
Coke (wt%)	3.82–4.55	4.00	6.04	2.04	7.86	3.86	9.41	5.41
Cat. temp. (K)		710.6	734.0	23.4	753.2	42.6	769.6	59.0
Gas phase temp. (K)		706.3	729.1	22.8	748.0	41.7	764.1	57.8

Optimization results

Table 5 presents the riser exit values of this simulation along with those riser exit concentrations from the optimization cases.

The results for both optimization cases 1, 2 and 3, and base case simulation (this simulation, Figs. 3, 4) are presented in Table 5, showing the riser exit values of the six lumps; gas oil as feed, while gasoline, butylene, propylene, dry gas and coke as products, and temperatures of the catalyst and gas phases. It compares the base case simulation results with the optimized cases 1, 2 and 3.

In the optimisation case 1, as propylene is maximized, the decision variable (catalyst mass flow rate) was set to be optimized between 20 and 500 kg/s, while gas oil temperature, T_g, was between 520–800 K and catalyst temperature, T_c, between 700 and 1000 K. The gas oil mass flow rate was fixed at 51.8 kg/s. The maximized value of propylene is 8.93 wt% at C/O ratio of 5.44 (gas oil mass flow rate is 51.8 kg/s and catalyst mass flow rate is 282.0 kg/s). The absolute difference between the maximized value and this simulation is 4.34 wt%, an increase from 4.59 to 8.93 wt%.

The optimized catalyst mass flow rate is 282.0 kg/s; it is a 47.72% increase on the 190.9 kg/s base case simulation. This increase produced results consistent with the riser hydrodynamics where increase in mass flow rate of catalyst can result in an increase in the reaction temperature and consequent yield of intermediate products [9, 19, 56]. There is 3.81 and 3.89% increase in the temperatures of the gas phase and catalyst, respectively, which in turn causes the increase in the yield of a difference of 5.26 wt% of dry gas from 1.55 wt% at C/O ratio of 3.69–6.81 wt% at C/O ratio of 5.44. Similarly, the yield of butylene has a difference of 5.10 wt% from 9.39 wt% at C/O ratio of 3.69–14.49 wt% at C/O ratio of 5.44. Due to increase in C/O and temperature of reaction, more gas oil cracks, a further 12.02 wt% was achieved from 26.11 wt% at C/O ratio of 3.69–14.09 wt% at C/O ratio of 5.44. This is also a reason for more yield of propylene and other intermediate products; butylene and dry gas. Gasoline also cracks in a secondary reaction and depletes from 51.36 wt% at C/O ratio of 3.69–43.68 wt% at C/O ratio of 5.44 giving rise to a loss of 7.68 wt%, this secondary reaction was also observed in the literature [57]. In optimization case 1, at C/O ratio of 5.44, 9.00 wt% of coke was deposited on the catalyst, against 4.00 wt% at C/O

Table 5 Propylene optimization results for cases 1, 2 and 3 and simulation results

Lump	Riser optimization output (wt%)						
	Current simulation	Case 1	Difference	Case 2	Difference	Case 3	Difference
	$C/O = 3.69$	$C/O = 5.44$	1.75	$C/O = 5.48$	1.79	$C/O = 5.45$	1.76
Gas oil (wt%)	26.11	14.09	− 12.02	14.06	− 12.05	14.07	− 12.04
Gasoline (wt%)	51.36	43.68	− 7.68	43.64	− 7.72	43.65	− 7.71
Butylene (C_4's) (wt%)	9.39	14.49	5.10	14.50	5.11	14.50	5.11
Propylene (C_3's) (wt%)	4.59	8.93	4.34	8.93	4.34	8.95	4.36
Dry gas (wt%)	1.55	6.81	5.26	6.85	5.30	6.83	5.28
Coke (wt%)	4.00	9.00	5.00	9.00	5.00	9.01	5.01
Cat. temp. (K)	710.6	737.7	27.1	738.5	27.9	737.7	27.1
Gas phase temp. (K)	706.3	733.8	27.5	734.2	27.9	733.8	27.5

ratio of 3.69 leading to an addition of 5.00 wt% of coke on catalyst. It is also a consequence of increased C/O ratio and reaction temperature. This increase in coke on catalyst may lead to high deactivation of the catalyst, which is not desirable, however, regeneration of the catalyst can be achieved and any eventual consequence is compensated by the much increase in the yield of propylene achieved.

Optimization cases 2 and 3 present similar outcomes as optimization case 1 because their optimum C/O ratios are quite similar; 5.44, 5.48 and 5.45 for cases 1, 2 and 3, respectively, with an absolute average difference of 0.016. This very slight difference is responsible for the slight average variation of 0.01 wt% in the riser outputs for the six lumps.

The optimisation case 2 has its decision variable changed from the mass flow rate of catalyst in case 1 to mass flow rate of gas oil. The gas oil mass flow rate was set to be optimized between 20 and 500 kg/s, while gas oil temperature, T_g, between 520 and 800 K and catalyst temperature, T_c, between 700 and 1000 K. The catalyst mass flow rate was fixed at 190.9 kg/s. The optimized gas oil mass flow rate is 34.86 kg/s, which is a 32.7% decrease on the 51.8 kg/s of the base case simulation and corresponds to C/O of 5.48, an increase of C/O ratio of 0.04 compared with the C/O ratio of optimization case 1. This result, as in case 1, is consistent with the riser hydrodynamics where increase in C/O results in increase in the reaction temperature and yield of intermediate products [7, 56]. There is 3.90 and 3.95% increase in the temperatures of the gas phase and catalyst, respectively. The increase in temperature in cases 1 and 2 is very similar because only C/O ratio difference of 0.04 between cases 1 and 2 exists, which even though the optimized conditions in case 2 increased the maximum value of propylene by 94.55% the same as case 1 compared with the simulation value of 4.59 wt%; there is no difference between the values of maximized propylene (8.93 wt%) between cases 1 and 2. Similarly, the yield of butylene and dry gas increased, respectively, by 5.11 and 5.26 wt% due to an increase in C/O ratio of 1.79 (C/O of 3.69–5.48). The amount of coke deposited in case 2 is as in case 1, which is 9.00 wt%. Since maximizing propylene is the main aim of this work, and cases 1 and 2 could achieve the same value of 8.93 wt%, any of the operating conditions of cases 1 or 2 can be used for optimal operation of the riser to produce optimum value of propylene, however, case 2 is preferable because of the difference of C/O ratio of 0.05.

The optimisation case 3 used two decision variables, unlike cases 1 and 2. These were gas oil and catalyst mass flow rates. The gas oil mass flow rate was set to be optimized between 20 and 500 kg/s as in case 1, and the catalyst mass flow rate was also set to be optimized between 20 and 500 kg/s as in case 2. The gas oil temperature, T_g, was set between 520 and 800 K and catalyst temperature, T_c, between 700 and 1000 K.

The optimized gas oil and catalyst mass flow rates are 53.4 and 290.8 kg/s, respectively, showing a 3.09% increase on the 51.8 kg/s base case condition for gas oil mass flow rate and 52.33% increase on the 190.9 kg/s base case condition for catalyst mass flow rate. These optimized flow rates correspond to a C/O of 5.45, an increased C/O of 1.74 on the base case simulation bringing about a 94.99% increase in propylene yield from 4.59 to 8.95 wt%. There is a slight increase of 0.05 wt% of propylene in case 3 over cases 1 and 2, which represents a 0.44% increase. This increase makes optimization case 3 most preferable because any small improvement to the yield of products in FCC unit amounts to great profitability. In general, the maximized value of propylene is 8.95 wt% achieved at C/O ratio of 5.45, even though, an average of 7.70 wt% of gasoline is lost due to secondary reaction with much coke deposited on the catalyst.

It is observed that the improved yield of propylene is accompanied with increase in some undesirable products such as dry gas and butylene as well as its isomer. It also increased catalyst deactivation. However, FCC units can be modified or operated in a mode shift to produce propylene with less of the aforementioned consequences. This could be achieved by the harmonious combination of the catalyst, temperature, C/O ratio, time, coke make, and hydrocarbon partial pressure [7].

An industrial size conventional FCC riser is simulated in this work to maximize the yield of propylene as a separate lump. The common view is where experimental works were carried out at specific temperature in fixed bed reactors, and propylene mostly considered as part of a general lump of olefins. Instead of using catalyst additives to improve the yield, only the operational conditions of the riser were used in this work. However, it is recommended that the use of both improved catalyst and optimum operating conditions will greatly increase the yield of propylene.

Conclusions

In this work, optimization of the FCC riser has been carried out using a detailed riser process model of a six-lumped kinetic model to maximize the conversion of gas oil to propylene, which is a major building block for the polypropylene production. Parameter estimation was also done to estimate the kinetic variables useful in the model used in this simulation. It is a steady state optimization carried out on a FCC riser and the following were found:

- In the case 1 optimization, the maximum value of propylene obtained is 8.93 wt% at optimal value of 282.0 kg/s catalyst mass flow rate. Compared with the base case

simulation value of 4.59 wt% propylene yield, the maximized value shows an increase by 95%.

- Likewise, in the case 2 optimization, the maximum value of propylene obtained is the same 8.93 wt% at optimal value of 34.86 kg/s gas oil mass flow rate. When it is compared with the base case simulation value of 4.59 wt% propylene yield, the maximized value shows an increase by 95%, as in case 1.
- When the two optimal values of 290.8 kg/s mass flow rate of catalyst and 53.4 kg/s mass flow rate of gas oil were obtained in case 3, the maximized propylene yield is 8.95 wt%, slightly higher than cases 1 and 2. When it is compared with the base case simulation value of 4.59 wt% propylene yield, the maximized value shows an increase by 95%.
- New kinetic parameters (frequency factor, activation energies and heat of reactions) were estimated for and used with a six-lumped kinetic model with a separate propylene lump. The yields of the six lumps fall within the range of yields presented in the literature.
- The optimization in all three cases (cases 1, 2 and 3) was achieved at C/O ratios of 5.44, 5.48 and 5.45, respectively. C/O ratio 5.45 gave the higher maximum value of propylene, hence the riser is required to operate at a minimum C/O ratio of 5.44 if optimal operation of the riser is required to maximize propylene yield.

Appendix

Table 6 and Eqs. (71)–(92) are correlations of physical and transport parameters adopted from the literature [2, 19].

Table 6 Distillation coefficients

Volume % distilled	a	b
10	0.5277	1.0900
30	0.7429	1.0425
50	0.8920	1.0176
70	0.8705	1.0226
90	0.9490	1.0110

The distillation coefficient used in this simulation is based on the 10, 50 and 90 vol% as used in Ancheyta and Rogelio [15].

Heat capacity of gas, C_{pg}, is

$$C_{pg} = \beta_1 + \beta_2 T_g + \beta_3 T_g^2, \tag{71}$$

where $\beta_1, \beta_2, \beta_3$ and β_4, the catalyst decay constants, given as

$$\beta_1 = -1.492343 + 0.124432K_f + \beta_4\left(1.23519 - \frac{1.04025}{S_g}\right), \tag{72}$$

$$\beta_2 = (-7.53624 \times 10^{-4})$$
$$\left[2.9247 - (1.5524 - 0.05543K_f)K_f + \beta_4\left(6.0283 - \frac{5.0694}{S_g}\right)\right], \tag{73}$$

$$\beta_3 = (1.356523 \times 10^{-6})(1.6946 + 0.0884\beta_4), \tag{74}$$

$$\beta_4 = \left[\left(\frac{12.8}{Kf} - 1\right)\left(1 - \frac{10}{Kf}\right)(S_g - 0.885)(S_g - 0.7)(10^4)\right]^2$$
$$\text{for } 10 < Kf < 12.8. \tag{75}$$

Else $\beta_4 = 0$ for all other cases
Kf is the Watson characterization factor written as

$$Kf = \frac{(1.8T_{MeABP})^{\frac{1}{3}}}{S_g}, \tag{76}$$

where M_{wg} is the molecular weight of the gas and can be calculated using

$$M_{wg} = 42.965\left[\exp\left(2.097 \times 10^{-4}T_{MeABP} - 7.787S_g + 2.085 \times 10^{-3}T_{MeABP}S_g\right)\right](T_{MeABP}^{1.26007}S_g^{4.98308}), \tag{77}$$

$$T_{MeABP} = T_{VABP} - 0.5556\exp[-0.9440 - 0.0087 \times (1.8T_{VABP} - 491.67)^{0.6667} + 2.9972(Sl)^{0.3333}, \tag{78}$$

where T_{VABP} is the volume average boiling temperature and (Sl) is the slope given as

$$(Sl) = 0.0125(T_{90ASTM} - T_{10ASTM}), \tag{79}$$

$$T_{VABP} = 0.333(T_{10ASTM} + T_{50ASTM} + T_{90ASTM}). \tag{80}$$

The ASTM D86 distillation temperatures are calculated using

$$T_{10ASTM} = a_{10}^{-\frac{1}{b_{10}}}\left(T_{10TBP}\right)^{\frac{1}{b_{10}}}, \tag{81}$$

$$T_{50ASTM} = a_{50}^{-\frac{1}{b_{50}}}\left(T_{50TBP}\right)^{\frac{1}{b_{50}}}, \tag{82}$$

$$T_{90\text{ASTM}} = a_{90}^{-\frac{1}{b_{90}}} \left(T_{90\text{TBP}}\right)^{\frac{1}{b_{90}}}, \tag{83}$$

where a_i and b_i are the distillation coefficients (Table 6) and $T_{i\text{TBP}}$ is the TBP distillation temperature.

Interface heat transfer coefficient between the catalyst and gas phases, h_p,

$$h_p = 0.03 \frac{K_g}{d_c^{\frac{2}{3}}} \left[\frac{|(v_g - v_c)|\rho_g \varepsilon_g}{\mu_g}\right]^{\frac{1}{3}}. \tag{84}$$

Thermal conductivity of hydrocarbons

$$K_g = 1 \times 10^{-6}(1.9469 - 0.374M_{\text{wm}} + 1.4815 \\ \times 10^{-3}M_{\text{wm}}^2 + 0.1028T_g), \tag{85}$$

where M_{WM} is the mean molecular weight of the combined catalyst and gas

$$M_{\text{WM}} = \frac{1}{\left(\frac{y_{\text{go}}}{M_{\text{wgo}}} + \frac{y_{\text{gl}}}{M_{\text{wgl}}} + \frac{y_{\text{C4}}}{M_{\text{wC4}}} + \frac{y_{\text{C3}}}{M_{\text{wC3}}} + \frac{y_{\text{dg}}}{M_{\text{wdg}}} + \frac{y_{\text{ck}}}{M_{\text{ck}}}\right)} \tag{86}$$

$$M_{\text{wgo}} = M_{\text{wg}} \tag{87}$$

$$M_{\text{dg}} = 0.0146M_{\text{wH}_2} + 0.4161M_{\text{wC}_1} + 0.5693M_{\text{wC}_2}. \tag{88}$$

The viscosity of the gas (Table 7)

$$\mu_g = 3.515 \times 10^{-8}\mu_{\text{pr}}\frac{\sqrt{M_{\text{WM}}P_{\text{pc}}^{\frac{2}{3}}}}{T_{\text{pc}}^{\frac{1}{6}}}, \tag{89}$$

$$\mu_{\text{pr}} = 0.435 \exp\left[\left(1.3316 - T_{\text{pr}}^{0.6921}\right)P_{\text{pr}}\right]T_{\text{pr}} + 0.0155, \tag{90}$$

$$T_{\text{pc}} = 17.1419\left[\exp\left(-9.3145 \times 10^{-4}T_{\text{MeABP}} \\ -0.5444S_g + 6.4791 \times 10^{-4}T_{\text{MeABP}}S_g\right)\right] \\ \times T_{\text{MeAB}}^{-0.4844}S_g^{4.0846}, \tag{91}$$

Table 7 Tuned coefficients for $0.2 \leq P_{\text{pr}} \leq 3$ [22]

Coefficient	Tuned coefficient
A1	2.827793
A2	−0.4688191
A3	−1.262288
A4	−1.536524
A5	−4.535045
A6	0.06895104
A7	0.1903869
A8	0.6200089
A9	1.838479
A10	0.4052367
A11	1.073574

Table 8 Specifications of constant parameters and differential variables at $x = 0$

Variable	Value
Riser height, L (m)	30
D riser diameter (m)	1.0
$T_g(0)$ (temperature of gas oil, K)	523
$T_c(0)$ (temperature of gas catalyst, K)	971
FF_c (catalyst mass flow rate, kg/s)	190.9
FF_g (gas oil mass flow rate, kg/s)	51.8
$y_{\text{gl}}(0)$ mass fraction of gasoline	0.0
$y_{\text{dg}}(0)$ mass fraction of dry gas	0.0
$y_{\text{C4}}(0)$ mass fraction of butylene	0.0
$y_{\text{C3}}(0)$ mass fraction of propylene	0.0
$y_{\text{ck}}(0)$ mass fraction of coke	0.0
M_{wck} molecular weight coke (kg/k mol)	14.4
M_{wH_2} molecular weights of hydrogen (kg/k mol)	2
M_{wC_1} molecular weights of methane (kg/k mol)	16
M_{wC_2} molecular weights of ethane (kg/k mol)	30
M_{wC_3} molecular weights of propane (kg/k mol)	44
M_{wC_4} molecular weights of butane (kg/k mol)	58
g, acceleration due to gravity (m/s²)	9.8
R, ideal gas constant (kPa m3/kg mol K)	8.3143

$$P_{\text{pc}} = 4.6352 \times 10^6\left[\exp\left(-8.505 \times 10^{-3}T_{\text{MeABP}} \\ -4.8014S_g + 5.749 \times 10^{-3}T_{\text{MeABP}}S_g\right)\right] \\ \times T_{\text{MeAB}}^{-0.4844}S_g^{4.0846}. \tag{92}$$

Table 9 Catalyst and feed properties

Variable	Value
Han and Chung [19]	
d_c (average particle diameter, m)	0.00007
C_{ckCL1} (Coke on catalyst, wt%)	0.001
α_{c0} (pre-exponential factor of α_c)	0.000011
α_{c*} (catalyst deactivation coefficient)	0.1177
C_{pc} (heat capacity of catalyst, kJ/kg K)	1.15
S_c (average sphericity of catalyst particles)	0.72
E_c catalyst activation energy (kJ/kg mol)	49,000
Ancheyta and Rogelio [15]	
ρ_c (density of catalyst, kg/m³)	890
API	24
S_g (specific gravity)	0.91
$T_{10\text{TBP}}$ TBP distilled 10 volume%, K	619
$T_{50\text{TBP}}$ TBP distilled 50 volume%, K	706
$T_{90\text{TBP}}$ TBP distilled 90 volume%, K	790
Paraffinics (wt%)	61.0
Naphthenics (wt%)	19.3
Aromatics (wt%)	19.6
R_{AN} (aromatics/naphthenes in liquid feedstock)	1.02

Table 8 summarizes the variables, feed and catalyst characteristic and other parameters used in this simulation. Most of the parameters were obtained from the industry and literature [19, 20, 58] (Table 9).

References

1. Ahsan M (2015) Prediction of gasoline yield in a fluid catalytic cracking (FCC) riser using k-epsilon turbulence and 4-lump kinetic models: a computational fluid dynamics (CFD) approach. J King Saud Univ Eng Sci 27:130–136
2. Han I-S, Chung C-B (2001) Dynamic modeling and simulation of a fluidized catalytic cracking process. Part I: process modeling. Chem Eng Sci 56:1951–1971
3. Xiong K, Lu C, Wang Z, Gao X (2015) Quantitative correlations of cracking performance with physiochemical properties of FCC catalysts by a novel lump kinetic modelling method. Fuel 161:113–119
4. Khanmohammadi M, Amani S, Garmarudi AB, Niaei A (2016) Methanol-to-propylene process: perspective of the most important catalysts and their behavior. Chin J Catal 37:325–339
5. Li C, Yang C, Shan H (2007) Maximizing propylene yield by two-stage riser catalytic cracking of heavy oil. Ind Eng Chem Res 46:4914–4920
6. Berrouk AS, Pornsilph C, Bale SS, Du Y, Nandakumar K (2017) Simulation of a large-scale FCC riser using a combination of MP-PIC and four-lump oil-cracking kinetic models. Energy Fuels 31:4758–4770
7. Akah A, Al-Ghrami M (2015) Maximizing propylene production via FCC technology. Appl Petrochem Res 5:377–392
8. Liu H, Zhao H, Gao X, Ma J (2007) A novel FCC catalyst synthesized via in situ overgrowth of NaY zeolite on kaolin microspheres for maximizing propylene yield. Catal Today 125:163–168
9. John YM, Patel R, Mujtaba IM (2017) Maximization of gasoline in an industrial fluidized catalytic cracking unit. Energy Fuels 31:5645–5661
10. Almeida NE, Secchi AR (2011) Dynamic optimization of a FCC converter unit: numerical analysis. Braz J Chem Eng 28:117–136
11. Khandalekar PD (1993) Control and optimization of fluidized catalytic cracking process. Texas Tech University, Lubbock
12. Haiyan L, Liyuan C, Baoying W, Yu F, Gang S, Xaojun B (2012) In-situ synthesis and catalytic properties of ZSM-5/rectorite composites as propylene boosting additive in fluid catalytic cracking process. Chin J Chem Eng 20:158–166
13. Inagaki S, Takechi K, Kubota Y (2010) Selective formation of propylene by hexane cracking over MCM-68 zeolite catalyst. Chem Commun 46:2662
14. Usman A, Siddiqui MAB, Hussain A, Aitani A, Al-Khattaf S (2017) Catalytic cracking of crude oil to light olefins and naphtha: experimental and kinetic modeling. Chem Eng Res Des 120:121–137
15. Ancheyta JRJ, Rogelio S (2002) Kinetic modeling of vacuum gas oil catalytic cracking. Revista de la Sociedad Química de México 46:38–42
16. Aitani A, Yoshikawa T, Ino T (2000) Maximization of FCC light olefins by high severity operation and ZSM-5 addition. Catal Today 60:111–117
17. Knight J, Mehlberg R (2011) Maximize propylene from your FCC unit. Hydrocarb Process 90:91–95
18. Parthasarathi RS, Alabduljabbar SS (2014) HS-FCC high-severity fluidized catalytic cracking: a newcomer to the FCC family. Appl Petrochem Res 4:441–444
19. Han I-S, Chung C-B (2001) Dynamic modeling and simulation of a fluidized catalytic cracking process. Part II: property estimation and simulation. Chem Eng Sci 56:1973–1990
20. John YM, Patel R, Mujtaba IM (2017) Modelling and simulation of an industrial riser in fluid catalytic cracking process. Comput Chem Eng 106:730–743
21. Ali H, Rohani S, Corriou JP (1997) Modelling and control of a riser type fluid catalytic cracking (FCC) unit. Chem Eng Res Des 75:401–412
22. Heidaryan E, Moghadasi J, Rahimi M (2010) New correlations to predict natural gas viscosity and compressibility factor. J Petrol Sci Eng 73:67–72
23. Mujtaba IM (2012) Use of various computational tools and gPROMS for modelling simulation optimisation and control of food processes. In: Ahmed J, Rahman MS (eds) Handbook of food process design, vol 1. Wiley-Blackwell, Hoboken
24. Jarullah AT, Awad NA, Mujtaba IM (2017) Optimal design and operation of an industrial fluidized catalytic cracking reactor. Fuel 206:657–674
25. John YM, Patel R, Mujtaba IM (2017) Optimization of fluidized catalytic cracking unit regenerator to minimize CO_2 emissions. Chem Eng Trans 57:1531–1536
26. Meng X, Xu C, Gao J, Li L (2006) Catalytic pyrolysis of heavy oils: 8-lump kinetic model. Appl Catal A 301:32–38
27. Meng X, Xu C, Gao J, Li L (2005) Studies on catalytic pyrolysis of heavy oils: reaction behaviors and mechanistic pathways. Appl Catal A 294:168–176
28. Naik DV, Karthik V, Kumar V, Prasad B, Garg MO (2017) Kinetic modeling for catalytic cracking of pyrolysis oils with VGO in a FCC unit. Chem Eng Sci 170:790–798
29. Hussain AI, Aitani AM, Kubů M, Čejka J, Al-Khattaf S (2016) Catalytic cracking of Arabian Light VGO over novel zeolites as FCC catalyst additives for maximizing propylene yield. Fuel 167:226–239
30. Du Y, Yang Q, Zhang C, Yang C (2015) Ten-lump kinetic model for the two-stage riser catalytic cracking for maximizing propylene yield (TMP) process. Appl Petrochem Res 5:297–303
31. Ancheyta-Juarez J, Murillo-Hernandez JA (2000) A simple method for estimating gasoline, gas, and coke yields in FCC processes. Energy Fuels 14:373–379
32. Yu-Chun Z, Zhen-Bo W, You-Hai J, Zhi-He L, Wei-Ming Y (2017) Kinetic study of catalytic cracking on the effect of reaction parameters in short-contact cyclone reactors. Chem Eng Res Des 119:188–197
33. Dobre TG, Marcano JGS (2007) Chemical engineering modelling simulation and similitude. Wiley-VCH Verlag GmbH & Co. KGaA, Weinheim
34. Soroush M (1997) Nonlinear state-observer design with application to reactors. Chem Eng Sci 52:387–404
35. Soroush M (1998) State and parameter estimations and their applications in process control. Comput Chem Eng 23:229–245
36. Tatiraju S, Soroush M (1997) Nonlinear state estimation in a polymerization reactor. Ind Eng Chem Res 36:2679–2690
37. Muske KR, Rawlings JB (1995) Nonlinear moving horizon state estimation. Kluwer Academic Publisher, Dordrecht
38. Robertson DG, Lee JH, Rawlings JB (1996) A moving horizon-based approach for least-squares estimation. AIChE 42:2209–2224
39. Jarullah AT, Mujtaba IM, Wood AS (2011) Kinetic parameter estimation and simulation of trickle-bed reactor for hydrodesulfurization of crude oil. Chem Eng Sci 66:859–871
40. Tjoa IB, Biegler LT (1992) Reduced successive quadratic programming strategy for errors-in-variables estimation. Comput Chem Eng 16:523–533
41. gPROMS (2013) Model validation guide. Process Systems Enterprise Limited, London

42. Ancheyta-Juárez J, Lopez-Isunza F, Aquilar-Rodriquez E, Moreno-Mayorga JC (1997) A strategy for kinetic parameter estimation in the fluid catalytic cracking process. Ind Eng Chem Res 36:5170–5174

43. Ancheyta-Juárez J, Sotelo-Boyás R (2000) Estimation of kinetic constants of a five-lump model for fluid catalytic cracking process using simpler sub-models. Energy Fuels 14:1226–1231

44. Ancheyta-Juárez J, López-Isunza F, Aquilar-Rodriquez E (1999) 5-Lump kinetic model for gas oil cracking. Appl Catal A Gen 177:227–235

45. Kasat RB, Kunzru D, Saraf DN, Gupta SK (2002) Multiobjective optimization of industrial FCC units using elitist nondominated sorting genetic algorithm. Ind Eng Chem Res 41:4765–4776

46. Zhou X, Yang B, Yi C, Yuan J, Wang L (2010) Prediction model for increasing propylene from FCC gasoline secondary reactions based on Levenberg–Marquardt algorithm coupled with support vector machines. J Chemom 24:574–583

47. Maadhah AG, Fujiyama Y, Redhwi H, Abul-Hamayel M, Aitani A, Saeed M, Dean C (2008) A new catalytic cracking process to maximize refinery propylene. Arab J Sci Eng 33:17–28

48. León-Becerril E, Maya-Yescas R, Salazar-Sotelo D (2004) Effect of modelling pressure gradient in the simulation of industrial FCC risers. Chem Eng J 100:181–186

49. Sadeghbeigi R (2012) Fluid catalytic cracking handbook. In: An expert guide to the practical operation, design, and optimization of FCC units, 3rd edn. The Boulevard, Oxford

50. Dupain X, Gamas ED, Madon R, Kelkar CP, Makkee M, Moulijn JA (2003) Aromatic gas oil cracking under realistic FCC conditions in a microriser reactor. Fuel 82:1559–1569

51. Moustafa TM, Froment GF (2003) Kinetic modeling of coke formation and deactivation in the catalytic cracking of vacuum gas oil. Ind Eng Chem Res 42:14–25

52. Gupta RK, Kumar V, Srivastava VK (2007) A new generic approach for the modeling of fluid catalytic cracking (FCC) riser reactor. Chem Eng Sci 62:4510–4528

53. Lan X, Xu C, Wang G, Wu L, Gao J (2009) CFD modeling of gas–solid flow and cracking reaction in two-stage riser FCC reactors. Chem Eng Sci 64:3847–3858

54. Farshi A, Shaiyegh F, Burogerdi SH, Dehgan A (2011) FCC process role in propylene demands. Pet Sci Technol 29:875–885

55. Souza JA, Vargas JVC, von Meien OF, Martignoni W, Amico SC (2006) A two-dimensional model for simulation, control, and optimization of FCC risers. AIChE J 52:1895–1905

56. Akah A, Al-Ghrami M, Saeed M, Siddiqui MAB (2016) Reactivity of naphtha fractions for light olefins production. Int J Ind Chem 8:221–233

57. Scott BJ, Adewuyi YG (1996) Effects of high temperature and high ZSM-5 additive level on FCC olefins yields and gasoline composition. Appl Catal A 134:247–262

58. Ahari JS, Farshi A, Forsat K (2008) A mathematical modeling of the riser reactor in industrial FCC unit. Pet Coal 50:15–24

59. Tsuo YP, Gidaspow D (1990) Computation of flow patterns in circulating fluidized beds. AIChE 36:885